IOSR Journal Of Applied Physics (IOSR-JAP)
e-ISSN: 2278-4861.Volume 12, Issue 5 Ser. III (Sep. – Oct 2020), PP 40-47
www.Iosrjournals.Org

Surface Stability of Smectic Ferroelectric Liquid Crystal Mixture

M. A. Zaki Ewiss
Department of Physics, Faculty of Science, Cairo University, Giza, Egypt.

Abstract
Background*: This work is broadly motivated by the development of ferroelectric liquid crystal devices and the need to develop a basic understanding of these strategic materials' wetting properties.*
Materials and Methods: *This article studied the surface stability and wetting properties of the smectic C* ferroelectric liquid crystal mixture using highly polarized reflected optical microscopy. We used a homemade spin-coated machine to prepare the thin-film samples of smectic C* ferroelectric liquid crystal mixture on soft silicon dioxide substrate with a thickness of 300 nm and 600 nm. Images of the film texture caught on heating and cooling processes, with a heating rate of 0.5 ^{o}C/min.*
Results: *The results showed the following: a) the thin film samples composed from multilayer, b) in both film thickness samples, the dewetting started a few degree ^{o}C below the bulk SmA to the isotropic phase transition temperature, c) in both thin-film surfaces, undulation was observed first, followed by spinoidal dewetting, d) above the isotropic phase, strongly depends on the value of the extracted contact angle of the formed sessile droplets with temperature was found and e) on cooling, the value of the contact angle remained constant, and the droplets remained until reached the re-crystalline phase. Attempts were made to extract the values of the tension surface length using the modified Young equation. These values monotonically decreased by increasing the temperature.*
Conclusion: *In conclusion, the FLC mixture's surface under consideration was stable by increasing the temperature within the SmC* and SmA phases. The dewetting observed above the SmA –I phase transition temperature. The first-order wetting transition characterizes these thin films.*
Keywords: *Liquid crystal, thin-film, wetting properties, surface undulation, anchoring force, contact angle, tension surface length*

Date of Submission: 10-10-2020 Date of Acceptance: 26-10-2020

I. Introduction

A wealth of information on liquid crystal materials' physical and chemical properties was reported[1-30]. The physical properties of the LC materials are intermediate between ordinary isotropic fluids and solid[1]. LC flow like liquids but also exhibits some properties of crystals. These materials are large, anisotropic, complex, and existed in different mesophases[1,2]. For technological applications, the physical properties of dielectric constants, elastic constants, viscosity, absorption spectra, transition temperatures, anisotropy, and LC's nonlinearity are interested[1-3].

Recently experimental and theoretical studies, of surface properties and the characteristics of solid surfaces interaction with liquids, are reviewed and discussed by Law and Zhao4 (including the references therein). This subject is a multidiscipline field with significant academic interests and tremendous applications in industry.

Unfortunately, the area of surface physics has been full of controversies and misconceptions. Many researchers paid attention to study the wetting properties of the nematic LC materials. The wetting phenomenon is related to the field of wetting and absorption of LC on a solid substrate, including the concepts of partial and complete wetting and partial and complete dewetting.

In this respect, many experimental approaches studied this phenomenon, such as optical microscopy, X-ray diffraction (XRD), atomic force microscopy (AFM), scanning polarizing force microscopy (SPFM), and ellipsometry techniques[1-34]. A better knowledge of liquid crystals' interfacial properties may lead to improvements in the performance of liquid crystal displays (LCDs) technology.

The fundamentals of understanding of the wetting in different systems are by measuring the contact angle. These angles are affected by many factors, such as heterogeneity, presence of surfactants, smoothness of the surface, and the line surface length. These factors strongly influenced the interpretation of their behaviour as a function of temperature. Zola et al.[6] presented information on the surface-induced phase separation and pattern formation at the isotropic interface in chiral nematic liquid crystals. Gunyakov et al.[7] investigated the temperature dependence of the significant anchoring energy for a nematic-ferroelectric interface. Zou et al.[8] reported experimental results on the line tension and structure of smectic liquid-crystal multilayer at the air-

water interface.

In 2018, Kaznacheev et al.[9] presented new results on the Biaxial potential of surface-stabilized ferroelectric liquid crystals(FLC's). They analyzed the biaxiality impact on the FLC alignment. In this experiment, the bistable or monostable structure formed in a surface stabilized FLC cell. Guo et al.[10] reviewed three electrooptic modes, including surface stabilized FLC, deformed helix ferroelectric, and electrically suppressed helix modes. Silvestre et al.[11] studied the wetting of cholesteric liquid crystals at a planar substrate theoretically. They found that the materials' wetting properties strongly depend on the anchoring conditions, which distort the liquid crystal layers.

Deshmukh and Malik[12] described a simple sessile drop technique for measuring polymer and nematic LC's surface tensions. Dhara et al.[13] studied the morphology transformation of the LC-5CB thin films coated on flat patterned PMMA substrate. The occurrence of the change from spin dewetted droplets to continuous films due to the increase of the solute concentration.

Thin films of the thermotropic LC- 5CB has been the subject to several thermal dewetting studies. The undulation on the surface of a 5CB thin-film appeared near the Nematic to Isotropic phase transition temperature[14-17]. Fukuda et al.[18] found an additional elastic force field within the LC thin film on a solid surface due to both the anisotropic anchoring at the substrate interface (weak planar anchoring) the strong homeotropic anchoring.

These factors result in a far more complex morphological evolution scenario in thin LC films, particularly during thermal annealing[14-19]. The behaviour of the free surface system and the molecular alignment within a confined liquid crystal system have been theoretically[20-25], and experimentally[26-29].

The alignment of liquid crystal molecules strongly depends on the boundary conditions, whether the LC film is confined between two plates or with a free surface on substrates. Uniform alignment of LC mesogens achieved on modified soft substrates. Using the scanning AFM and the rubbing process, this modification of soft polymeric substrates creates nano or microgrooves[30-35].

The LC layer's complex order and phase behaviour within a confined system strongly depend on the interplay. Research on surface characteristics of ferroelectric LC's (FLC's) has always been messy in literature. The wetting dynamic of these materials' formed microdroplets determined by surface tension, viscosity, and temperature for a given liquid crystal–solid interface. Studying the stability of ferroelectric liquid crystal (FLC) thin film on a solid substrate is of interest in many applications such as the optically addressed spatial modulators, semiconductors, FLC thin-film devices, and liquid crystal on silicon (LCOS) technologies[4].

Information on the wetting and dewetting characteristics of FLC mixture thin films are scarce in the literature. This article presents and discusses new experimental results concerning the commercial FLC mixture material's wetting properties and surface stability. This research is part of an intensive research program on ferroelectric liquid crystal's dynamical and electrical properties.

II. Experiment

This experiment studied the surface stability and the wetting properties of ferroelectric liquid crystal mixture—thin films prepared on a smooth silicon wafer substrate. Under consideration, the FLC sample was a commercial multi-compound mixture developed (by Mitsubishi Company, Japan with catalogue number NS1010) for analogue electrooptic applications). The liquid crystal research group at the University of Colorado, USA, delivered this material. From the datasheet provided, this strategic material has a spontaneous polarization of 102 nC/cm^{2,} and its molecules have a tilt angle of 28^{o} at room temperature (T = 25 ^{o}C). It shows an SmC* to SmA phase transition at T = 70 ^{o}C, and a temperature control unit (Instec model STC 200) with a precision of ± 0.1 ^{o}C. We illuminate the sample is by a white light beam emitted from a halogen lamp. This light first passes through the linear polarizer. After reflection from the sample's surface, the SmA to Isotropic (I) - phase transition occurred at T = 97 ^{o}C. The measurements performed using a high-resolution polarizing optical microscope (Olympus BX51TRF) equipped with a heating stage (Instec model HCS402). The sample's temperature stabilized by reflected light falls on a digital camera (Olympus model C-3040) coupled to a computer. Real-time images of the thin-film surfaces at specific temperatures were recorded and displayed on the monitor. A magnification lens of power 20x was used; the scale calibrated such that a 1 µm length on the sample is equivalent to 0.75 mm on display.

Thin films under consideration prepared at room temperature according to the following procedure:

- We used silicon wafers with a native oxide layer of 2 nm thicknesses (100 oriented, p- Boron doped) as a solid substrate.
- The wafers were then cut to about 1 cm^2 in size and cleaned with a snow jet of a cold CO_2 stream, which effectively removes the particulate and the organic contaminants, followed by ultrasonication in ethanol, acetone, and hexane, subsequently.
- The liquid crystal films were spin-casted onto the substrate from the hexane solution.

- We paid attention to control the thin film's thickness by the FLC's material concentration and the spin coater's spinning speed. The concentration of the NS1010 FLC mixture in the hexane solution was 11.6 g/l.
- The spinning speed was 2000 and 4000 revolutions per minute (rpm), corresponding to film thickness of 300 nm and 600 nm, respectively.
- The thickness after spun cast FLC the film was measured by using ZYGO

Maxim-GP 200 profile-meter, a general-purpose surface optical profiler, measures the microstructure and topography of surfaces in three dimensions. We used the light from a Halogen lamp incident on an interference filter of wavelength 611.4 nm (or 643 nm) with a full width at half maximum (FWHM) ≈3 -15 nm. Monochromatic light is filtered and falls on an optical cube beam splitter, which directs the light downwards to an interferometric objective (Michelson type) controlled by the Piezo-electric transducer phase stepping fringe. The light reflected from the test object returns through the interferometric objective lens and passes through the cube beam splitter to the camera to form interference fringes. We obtained all surface-related data using a computer and advanced texture analysis software. The instrument can measure step height up to 100 μm with 0.75% accuracy. In this experiment, we use the optical microscopy techniques to study the dewetting of the isotropic thin film-forming microscopic cap-shaped droplets on the silicon substrate surface for the prepared samples. Figure 1 shows the geometry of the cap-shaped droplet.

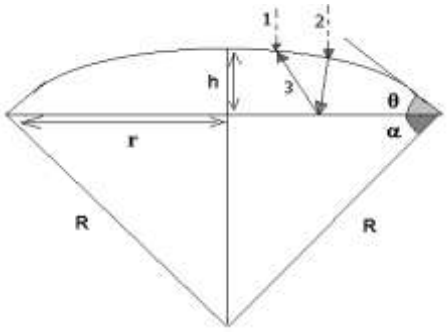

Figure 1: Sketch of a spherical cap-shaped droplet resting on a solid surface. The interference fringe is formed by the illuminating beam (1) and the reflected beam (3) originating from the illuminating beam (2). $2nh = (m+0.5)\lambda$, $R = (r2 + h2)/ 2h$, and $\cos\alpha = r/R$, since $\theta = 90-\alpha$.

This technique enabled us to measure small contact angles less than 10^o with an accuracy of $0.5^o - 1^o$, for droplets of average radii ranging from 1-100 μm, respectively. The radius (r) of each droplet was measured with an accuracy ± 0.01 μm for small droplets and ± 0.1 μm for big droplets.

We observe the wetting behaviour during the heating and cooling processes for all samples, with a rate of 0.5 ^{o}C/min started from room temperature. At a temperature of 130 ^{o}C, the measurement stopped to avoid the evaporation of the sample. Each droplet's contact angle is calculated by counting the number of the observed interference Newton rings and measuring each droplet's radius. From Figure (2), the height, h, of the droplet is given by[17]:

$$h = (m + 0.5)\left(\lambda/_{2n}\right) \quad (1)$$

where m is the order of the interference fringes (is the wavelength of the incident light, and n is the liquid crystal sample's refractive index. We calculate the contact angle θ of each droplet from the formula[17]:

$$\theta = 90^{\circ} - \cos^{-1}\left(2rh/_{(r^2 + h^2)}\right) \quad (2)$$

where r is the average radius of the spherical cap-shaped droplet.

III. Results and Discussion

In Figure 2 (a-i) and Figure 3(a-i) illustrate the evolution of the texture structure of the NS1010 ferroelectric liquid crystal mixtures thin films of thickness d= 300 nm (sample 1) and d = 600 nm (sample 2) at a different temperature, respectively. We investigate the samples' wetting behaviour during the heating and cooling processes with a heating (cooling) rate of 0.5 ^{o}C/min.

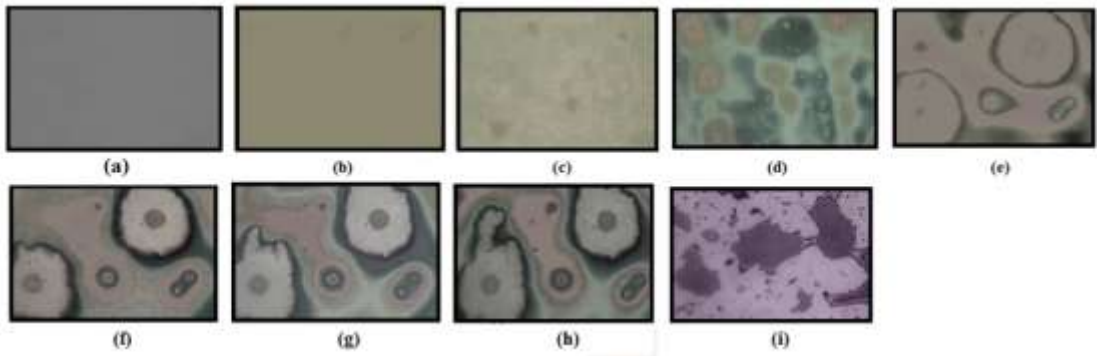

Figure 2: Images of the texture structure of NS1010 FLC mixture of thickness d = 300 nm at different temperature of values:
a) T = 28 ºC, b) T = 92 ºC, c) T = 94 ºC, d) T = 95 ºC, e) T = 97 ºC,
f) T = 100 ºC, g) T = 102 ºC, h) T = 108 ºC, i) T = 109 ºC

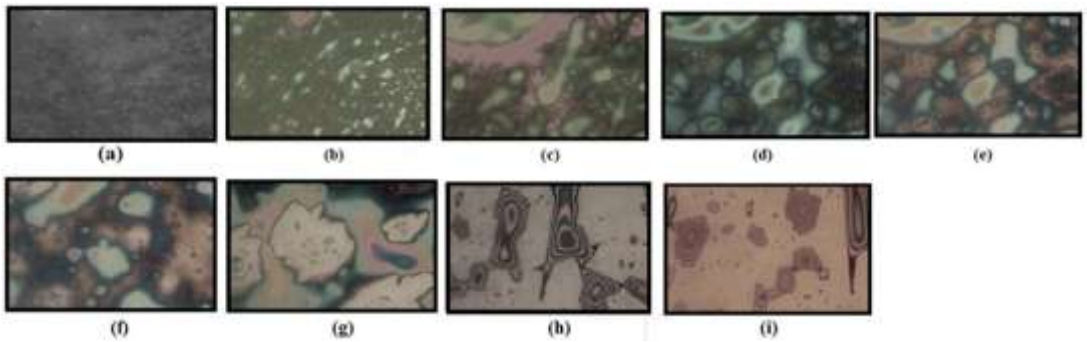

Figure 3: Images of the texture structure of NS1010 FLC mixture of thickness d = 600 nm at the different temperature of values:
a)T = 28 ºC, b) T = 92 ºC, c) T = 94 ºC, d) T = 95 ºC, e) T = 97 ºC,
f) T = 98.5 ºC, g) T = 100 ºC, h) T = 108 ºC, i) T = 111 ºC

As shown in Figure 2 (a, b) and Figure 3 (a, b) on the heating process, up to T = 90 ^{o}C, no variation in the film texture structure in both samples. Figure 2c and Figure 3c noticed that white spots appeared within the matrix of sample1 and sample2 at T = 94 ^{o}C and T = 92 ^{o}C, respectively. The size of these white spots increases by increasing the temperature. In Figure 2(d, e), and Figure 3(d, e), we observed surface undulation in both thin-film samples around T = 95 ^{o}C before reaching the Sm A - I phase transition temperature (at T_{SmA-I} = 97 ^{o}C). We may attribute this undulation to the change in anchoring conditions, thermal-induced surface instability, the viscosity gradient of the formed layers, and the tension surface length within each layer.

At T > 95 ^{o}C, a spinoidal dewetting occurred in both samples. In the thicker sample 2, this process was accompanied by heterogenous nucleation dewetting. The white spots rapidly grew as the liquid crystal material drifted from the inner surface, and a hole was formed. The drifted material was accumulated at the hole-boundary. Similar observations were reported, and theoretical attempts were made to explain this phenomenon[38-40]. In these reports, the nucleation and wetting near-surface spinodal in the binary mixture system was described. It was mentioned that when the system is in a metastable state, the decay towards equilibrium is governed by a nucleation process. In this case, the formation of the thermodynamically stable state starts with the nucleation of droplets. On the other hand, Bonn et al.[38] studied the formation and growth of wetting layers in the binary liquid mixture of cyclohexane-methanol. They observed that the nucleation probability decreases rapidly with increasing film thickness. Braun et al.[39] reported a theoretical model to explain the spinoidal dewetting of a nematic film, which is destabilized by Van Der Waals forces.

As shown in Figure 2 and Figure 3, the dewetting due to the formation of the sessile droplets in both sample1 (with film thickness d = 300 nm) and sample 2 (with film thickness d = 600 nm) occurs at temperature T = 100 ^{o}C and T = 108 ^{o}C, respectively. From equation (2), each droplet's contact angle (θ) was determined as

a function of temperature, using the microscopic method as discussed above. Here, the contact angle is dictated by the materials at the three-phase contact line rather than the contact area materials.

Figure 4 (a, b) shows the variation of θ versus the temperature for both samples. From Figure 4a, the value of θ reaches a maximum value of 5° at T = 120 °C for sample1 with film thickness d= 300 nm, and from Figure 4b, the value of θ becomes 7.8° at T=130 °C for sample 2 with film thickness d=600 nm. On cooling, a slight variation of the contact angle by 14% and 25% from its maximum value for Sample1 and Sample 2. The formation of a multilayer of the liquid crystal material under investigation and its mixture structure could be responsible for this effect. It is worth mentioning that, on cooling down to room temperature at T = 28 °C, the droplets are frozen, and rewetting doesn't occur.

It is known for a self-assembled monolayer of liquid crystal on a solid surface. The surface energies have often been based on the values of the contact angle. In such cases, the famous Young equation[40] may be used to describe the equilibrium force balance in the coexistence of three phases: a liquid drop resting on an underlying solid surface, in equilibrium with the saturated vapour.

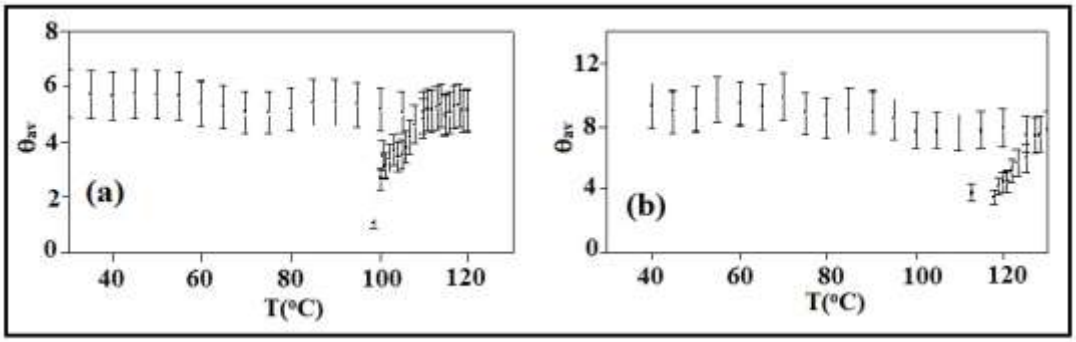

Figure 4: Variation of average contact angle θAV. with temperature during heating and cooling processes for: (a) Sample1 of d = 300 nm film thickness, (b) Sample2 of d = 600 nm film thickness.

The angle θ made by the surface of the drop at the point where it meets the underlying substrate satisfies the relation:

$$\cos\theta = {}^{(\gamma_{sv} - \gamma_{sl})}/_{\gamma_{lv}} \tag{3}$$

Where γ_{lv}, γ_{sl} and γ_{sv} are the surface energies per unit area of the liquid/vapour, solid/liquid, and solid/vapour interfaces, respectively. The inherent difficulty presented by Young's equation is related to the quantities γ_{sl} and γ_{sv}, which are not usually accessible in a direct experimental measurement[41].

For microscopic droplets, the contact angle is influenced by surface interactions, which will contribute an additional free energy per unit length or a line tension (τ) to the excess free energy of the microscopic droplet. So, an extra energy term is added to equation (3). Hence, for a tiny spherical cap-shaped droplet of contact angle (θ), we obtain the modified Young's equation, which can alternatively be written as[17]:

$$\gamma_{sv} = \gamma_{sl} + \gamma_{lv}\cos\theta + {}^{\tau}/_{R} \tag{4}$$

Or

$$\cos\theta = \cos\theta_{\infty} - {}^{\tau}/_{\gamma_{lv}R} \tag{5}$$

Where; θ is the contact angle of the microscopic droplet, θ_{∞} is Young's contact angle (i.e., the contact angle for an infinitely large droplet), $\lambda = \tau/\gamma_{sl}$ is called the tension surface length, τ is the contact line tension (which has the units of force (N)), γ_{vl} is the surface tension of the air/liquid crystal interface (N/μm), and R (μm) is the radius of curvature of the circular contact line.

Figure 5 (a, b) shows the variation of (cosθ) as a function of the droplet curvature (1/R) at different temperatures within the isotropic phase for sample1 and sample2, respectively. The results indicate that by increasing the temperature, the rate of relaxation for the contact angle is increased, and the final contact angle is decreased. This effect may be attributed to the FLC mixture content changes inside the droplet, anchoring conditions, the value of the surface tension, and the viscosity.

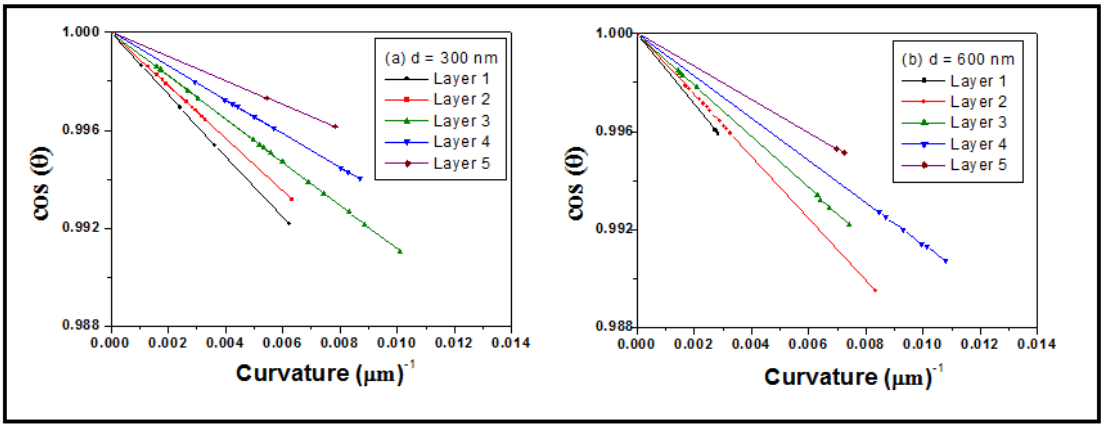

Figure 5: The relation between cosθ, and the droplet curvature (1/R) for a) Sample1 of d = 300 nm film thickness and b) Sample2 of d = 600 nm film thickness

Also, due to the evaporation effect, it is noticed that the number of the formed droplet decreases at 116 ^{o}C ≤T≤120 ^{o}C for sample1 (d=300 nm) and 122 ^{o}C ≤T≤130 ^{o}C for sample2 (d=600 nm). The curves in Figure 5 (a, b) represent the linear relation of equation (6), which characterizes the multilayer structure within the liquid crystal film matrix, as discussed above. The values of the tension surface length (λ) are determined from the slope of this linear relation for both samples and plotted versus the corresponding reduced temperature ($t = (T-T_w)/T_w$), as illustrated in Figure 6. It is worth noticing that the value of λ for both samples is monotonically decreased by increasing the isotropic phase's temperature. At $T=T_w$, it reaches its maximum value of λ_{max} = 1.32 μm for sample1 (film thickness d=300 nm) and λ_{max} = 2.2 μm for sample2 (film thickness d=600 nm). In the I- phase, far from the critical point, the surface's spatial delocalization leads to a usual negative slope (dλ/dt) <0, which is typical of isotropic liquids. The linear relation shown in Figure 6 indicates that the first-order wetting transition characterizes both samples. It is believed that the value (dλ/dt) may be responsible for the surface instability of the FLC mixture under consideration in the isotropic phase.

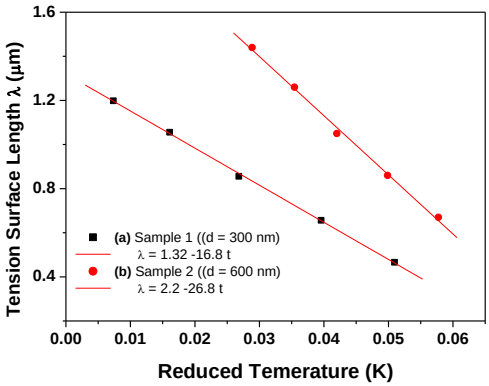

Figure 6: The relation between the tension surface lengths (λ in μm) as a function of the reduced temperature t = (T-Tw)/Tw for: a) Sample1 (d =300 nm) b) Sample2 (d = 600 nm)

As a limitation of the microscopic method, more experiment data such as measuring viscosity as a function of temperature, surface tension, determining the surface free energy, and the friction force between the liquid crystal layers are needed to explain this phenomenon.

IV. Conclusion

In this report, high resolution optical polarized microscopy technique is used to study the surface stability and the wetting properties of the commercial ferroelectric of liquid crystal mixture as a thin film spin-coated on the silicon wafer. This FLC mixture's surface was found stable by increasing the temperature within the SmC* and SmA phases. During the heating process undulation, and spinoidal dewetting has been observed at the SmA –I phase transition. These processes are accompanied by heterogenous nucleation dewetting, where the liquid crystal material drifted from the inner surface, and a hole was formed. The dewetting occurred above the isotropic phase, where the contact angle of the formed microdroplet was deduced as a function of

temperature. On the cooling process, the rewetting of the formed droplets did not occur. Attempts were made to apply the modified Young's equation. We found that the FLCmixture's thin-film comprises at least five layers, and the value of each layer's tension surface length was deduced. This value was found to decrease monotonically by increasing the temperature within the isotropic phase.

Acknowledgement

The author is indebted to Prof. N. Clark from the Liquid Crystal Group at the University of Colorado, the USA, for his active support and providing the liquid crystal material under consideration.

References

[1] P. G. De Gennes, J. Prost, The physics of liquid crystals, 2nd Ed., Oxford Science Publications; Oxford University Press**, (1993),** New York, N. Y., ISBN: 0-19-852024-7; xvi + 597 pages
[2] C. Khoo, Liquid crystals. 2nd Ed. Hoboken, New Jersey, USA: Wiley **(2007)**.
[3] C. Khoo, Nonlinear optics of liquid crystalline materials, Physics Reports; **(2009);** 471, pp: 221- 267.
[4] K. Y. Law, H. Zhao, Surface wetting: characterization, contact angle, and fundamentals, Springer International Publishing Switzerland, **(2016).**
[5] J. W. Goodby, P. J. Collings, T. Kato, C. Tschierske, H. F. Gleeson, P. Raynes, Handbook of liquid crystals, edited by, Weinheim, Wiley-VCH**, (2014)**.
[6] R. S. Zola, L. R. Evangelista, Y. C. Yang, D. K. Yang, Surface-induced phase separation and pattern formation at the isotropic interface in chiral nematic liquid crystals. Phys. Rev. Lett; **(2013)**,110057801(pp: 1-5).
[7] V. A. Gunyakov, A. M. Parshin, V. F. Shabanov, Temperature dependence of the effective anchoring energy for a nematic-ferroelectric interface. Eur. Phys. J**; (2006),** E20, pp: 467-473.
[8] L. Zou, J. Wang, P. Basnet, E. K. Mann, Line tension and structure of smectic liquid-crystal multilayers at the air-water interface. Phys Rev E Stat Nonlin. Soft Matter Phys.; **(2007)**; **76**, 031602, [pdf] arxiv.org, pp:1-21.
[9] V. Kaznacheev, P. P. Evgeny, V. Y. Rudyak, A. Khokhlov, Biaxial potential of surface-stabilized ferroelectric liquid crystals. Physical Review E, (2018); 97(4), 042703(pp: 1-12).
[10] Q. Guo, K. Yan, V. Chigrinov, H. Zhao, Tribelsky, M. Ferroelectric liquid crystals: physics and applications. Crystals, **(2019);** 9(9), pp: 470-491.
[11] N. M. Silvestre, M. C. F. Pereria, N. R. Bernardino, M. M. Tela da Gama, Wetting of cholestric liquid crystals. Eur. Phys**.; (2016)**; 39, pp: 13-19. Retrieved from: DOI: 10.1140/epje/i2016-16013-x
[12] R. R. Deshmukh, M. K. Malik, A method for estimating interfacial tension of liquid crystal embedded in polymer matrix forming PDLC. Wiley Periodicals, Inc. J. Appl. Polym. Sci.; **(2014);** 131, pp: 1-6.
[13] P. Dhara, N. Bhandaru, A. Das, R. Mukherjee, Transition from Spin Dewetting to continuous film in a spin coating of Liquid Crystal 5CB. Scientific Reports; **(2018);** 87169(pp: 1-9).
[14] D. van Efenterre, R. Ober, M. P. Valignat, A. M. Cazabat, Binary separation in very thin nematic films: thickness and phase coexistence. Phys. Rev. Lett; (2001); 87, 125701. Retrieved from: DOI: 10.1103/PhysRevLett.87.125701
[15] S. Schlagowski, K. Jacobs, S. Herminghaus, Nucleation-induced undulative instability in thin films of nCB liquid crystals. Europhys. Lett.; **(2002)**; 57, pp: 519–525.
[16] D. van Efenterre, M. P. Valignat, Stability of thin nematic films. Eur. Phys. J. E; **(2003**); 12, pp: 367–372.
[17] M. A. Zaki Ewiss, G. Nabil, S. Schlagowski, S. Herminghaus, Wetting behaviour of 5CB and 8CB and their binary mixtures above the isotropic transition. Liq. Cryst.; **(2004)**; 31, pp: 557–566.
[18] F. Vandenbrouck, M. P. Valignat, A. M. Cazabat, Thin nematic films: metastability and spinodal dewetting, Phys. Rev. Lett.; **(1999**), 82**,** pp: 2693–2696.
[19] P. Ziherl, R. Podgornik, S. Zumer, Wetting-driven Casimir force in nematic liquid crystals. Phys. Rev. Lett.; **(1999),** 82**,** pp:1189–1192.
[20] D. W. Berreman, Solid Surface Shape and the Alignment of an Adjacent Nematic Liquid Crystal. Phys. Rev. Lett.; **(1972),** 28, pp: 1683–1686.
[21] J. Fukuda, J. S. Gwag, M. Yoneya, H. Yokoyama, Theory of anchoring on a two-dimensionally grooved surface. Phys. Rev. E; **(2008),** 77**,** 011702. Retrieved from: https://doi.org/10.1103/PhysRevE.77.011702
[22] L. Cattaneo, J. Zhang, M. Zuiddam, M. Savoini, T. Rasing, Gaining control through frustration: two-fold approach for liquid crystal three-dimensional command layers. Nano Lett.; **(2014)**; 14, pp: 3903–3907.
[23] T. Shioda, B. Wen, C. Rosenblatt, Continuous nematic anchoring transition due to surface-induced smectic order. Phys. Rev. E; (2003); 67, 041706.
[24] J. Fukuda, M. Yoneya, H. Yokoyama, Surface-groove-induced azimuthal anchoring of a nematic liquid crystal: Berryman's model reexamined. Phys. Rev. Lett**.; (2007)**; 98(18), 187803.
[25] G. P. Sinha, B. Wen, C. L. Rosenblatt, Continuously controllable nematic pretilt from a vertical orientation. Appl. Phys. Lett.; **(2001**); 79, pp: 2543–2545.
[26] J. Stohr, et al. Liquid crystal alignment on carbonaceous surfaces with orientational order. Science; **(2001)**; 292, pp: 2299–2302.
[27] S. H. Ryu, D. K. Yoon, Molecular orientation of liquid crystals on topographic nanopatterns. ACS Appl. Mater. Interfaces; **(2016)**; 8, pp: 17707–17712.
[28] K. Ichimura, W. Suzuki, T. Seki, A. Hosoki, K. Aoki, Reversible change in alignment mode of nematic liquid crystals regulated photochemically by "command surfaces" modified with an azobenzene monolayer. Langmuir, **(1988)**; 4, pp: 1214–1216.
[29] S. H. Ryu, D. K. Yoon, Liquid crystal phases in confined geometries. Liq. Cryst.; **(2016)**; 43, pp: 1951–1972.
[30] M. Barmentlo, N. A. J. M. van Aerle, R. W. J. Hollering, J. P. M. Damen, Surface-induced liquid-crystal alignment studied by optical second-harmonic generation. J. Appl. Phys.; **(1992)**; 71, pp: 4799–4804.
[31] K. Sakamoto et al. Determination of the molecular orientation of very thin rubbed and unrubbed polyimide films. J. Appl. Phys.; **(1996)**; 80, pp: 431–439.
[32] R. Lin, J. A. Rogers, Molecular-scale soft imprint lithography for alignment layers in liquid crystal devices. Nano Lett.; **(2007)**; 7, pp: 1613–1621.
[33] Y. Yi, et al. Topographic-pattern-induced homeotropic alignment of liquid crystals. Phys. Rev. E; **(2009),** 79, 041701(pp:1-9).
[34] C. Anquetil-Deck, D. J. Cleaver, Nematic liquid-crystal alignment on stripe-patterned substrates. Phys. Rev. E; **(2010),** 82,031709.
[35] J. W. Cahn, Critical point wetting, Journal of Chemical Physics; **(1977);** 66 (8), pp: 3667-3672.

[36] J. Becker, G. Grün, R. Seemann, H. Mantz, K. Jacobs, K. R. Mecke, R. Blossey, Complex dewetting scenarios captured by thin-film models. Nature material; **(2003)**; 2, J. Becker, G. Grün, R. Seemann, H. Mantz, K. Jacobs, K. R. Mecke, R. Blossey, Complex dewetting scenarios captured by thin-film models. Nature material; **(2003)**; 2, PP: 59-63.
[37] D. Bonn, J. O. Indekeu, Nucleation and Wetting near Surface Spinodals, Phys. Rev. Lett.; **(1995);** 74, pp: 3844-3837.
[38] D. Bonn, E. Bertrand, J. Meunier, R. Blossey, Dynamics of Wetting Layer Formation. Phys. Rev. Lett; **(2000);** 84, pp: 4661-4.
[39] F. N. Braun, H. Yokoyama, Spinodal dewetting of a nematic liquid crystal film, Phys. Rev. E, **(2000);** 62, pp: 2974-6
[40] P. Somasundaran. [Ed], Encyclopedia of Surface, and Colloid Science. CRS, **(2006)**, Vol.4, Taylor, and Francis Group.
[41] M. K. Chaudhury, G. M. Whitesides, Direct measurement of interfacial interactions between semispherical lenses and flat sheets of poly (dimethylsiloxane) and their chemical derivatives, Langmuir; **(1991)**; 7, pp:1013-1025.

M. A. Zaki Ewiss, et. al. "Surface Stability of Smectic Ferroelectric Liquid Crystal Mixture." *IOSR Journal of Applied Physics (IOSR-JAP)*, 12(5), 2020, pp. 40-47.